Nanoscale

COMMUNICATION

View Article Online
View Journal | View Issue

Cite this: *Nanoscale*, 2019, **11**, 3794

Received 26th November 2018,
Accepted 6th February 2019

DOI: 10.1039/c8nr09547g

rsc.li/nanoscale

Visible light to switch-on desorption from goethite†

Anna Šutka,[a] Martin Järvekülg,[b] Karlis Agris Gross,[a] Mati Kook,[b] Tanel Käämbre,[b] Meeri Visnapuu,[b] Gregor Trefalt *[c] and Andris Šutka *[b,d]

Switching adsorption–desorption by visible light could provide the possibility for a wide range of applications that require controlled release-on-demand. Here, we demonstrate a visible-light controlled desorption behavior in aqueous suspensions for the first time. We observed cationic dye adsorption on amphoteric goethite α-FeOOH in the dark and release during visible light exposure at a pH value slightly over the isoelectric point of goethite. During this process, the dye does not degrade. Desorption is triggered by local heating due to light absorption in narrow band gap goethite, α-FeOOH.

The visible light triggered release of adsorbed ions/molecules from the surface of nanoparticles could open a wide range of novel applications including drug delivery, sedimentation, desalination, change in pH, optical devices based on ionic dyes and sensing.[1,2] Light can be further used to induce the mechanical response of materials[3,4] or fluorescence switching which is applicable in sensors and fluorescent logic devices.[5–7]

Access to this untapped abundant source of energy offers a safe, easy and readily accessible means to switch-on or switch-off different phenomena. This work will describe a new method for attaching molecules, for desorption by visible light. Specifically, we study the adsorption/desorption of methylene blue on goethite triggered by visible light. Such an approach could possibly be extended to other adsorbing molecules and therefore is potentially suitable for a variety of aforementioned applications.

Some release mechanisms include a tailored polymer to favor release, but most release triggers are coupled to nanoparticles that activate delivery.[1] The most eloquent release mechanism involves the change in the conformation of organic compounds, from one isomer to another after exposure to UV light,[2,3] thereby altering the molecule's adsorption affinity. This is restrictive to a limited number of transportable molecules. On a smaller scale, covalent bonds have been designed in stimuli-responsive surfaces for light exposure to activate the separation of drugs.[4] However, there are simpler approaches with functional nanoparticles to facilitate the release from a carrier.[1]

The functional particles in previous cases rely on nanoparticles to heat the polymer to promote delivery.[5–7] In the first mechanism, light absorbed in nanoparticles heats the nanoparticles, which shrinks the hydrogel and squeezes absorbed species from within its core.[5,6] The second approach uses metallic plasmonic nanoparticles, such as gold, to turn light into the heat for scission and desorption.[7] In our approach, the adsorption is promoted by the electrostatic interaction and release is triggered by visible light for a release from α-FeOOH nanowires.

Goethite α-FeOOH is an amphoteric oxide-hydroxide compound, which alters the surface charge sign and the charge density upon a change in pH of the aqueous solution.[8,9] Surface charging of goethite can be described by the equilibrium[9]

$$\mathrm{Fe\text{–}OH_2}^{+1/2} \leftrightarrow \mathrm{Fe\text{–}OH}^{-1/2} + \mathrm{H}^{+}$$

At a low pH, the surface is positively charged, but changes to a negative charge at a high pH. Surface charging on nanostructured goethite provides a large adsorption capacity for cationic dyes and metal cations, because of the favorable electrostatic interactions above the isoelectric point.[10] In addition to the aforementioned features, α-FeOOH is a narrow band gap semiconductor (a gap energy of 2 to 2.5 eV)[11] which allows for visible light absorption and subsequent triggered release.

This study investigates the influence of visible light irradiation on the desorption of methylene blue from

[a]*Biomaterials Research Laboratory, Institute of Inorganic Chemistry, Riga Technical University, P. Valdena 3/7, Riga, LV-1048, Latvia*
[b]*Institute of Physics, University of Tartu, Wilhelm Ostwald Str. 1, 50411 Tartu, Estonia. E-mail: andris.sutka@rtu.lv*
[c]*Department of Inorganic and Analytical Chemistry, University of Geneva, Sciences II, 30 Quai Ernest-Ansermet, 1205 Geneva, Switzerland. E-mail: gregor.trefalt@unige.ch*
[d]*Research Laboratory of Functional Materials Technologies, Riga Technical University, P. Valdena 3/7, 1048 Riga, Latvia*

†Electronic supplementary information (ESI) available. See DOI: 10.1039/c8nr09547g

α-FeOOH. The change in surface properties induced by light has been reported for goethite in the presence of H_2O_2,[8] siderophores[9] and polycarboxylic acids at low pH.[10] In the present work, methylene blue release has been observed without adding any promoters for goethite surface change in light. Goethite only requires low visible light exposure to facilitate desorption at pH values near the isoelectric point. We hypothesize that photogenerated electrons and holes recombine over the band gap of goethite nanoparticles and release the visible light energy as heat. This released heat in turn triggers desorption.

Goethite nanoparticles used for experiments were precipitated in water from 0.1 M iron(III) nitrate (98%, Sigma Aldrich) solution after adding a 0.4 M NaOH solution. Dark brown sediments were formed after adding the NaOH solution. The sediment was then stirred for 30 min and aged in a closed glass bottle for 72 h at 60 °C to facilitate the α-FeOOH formation. After synthesis, the light yellow sediment was washed by centrifugation 10 times, see Fig. S1.†

The microstructural features of the samples were studied by electron microscopy. Both scanning electron microscopy (SEM) and transmission electron microscopy (TEM) were used. The size of goethite nanocrystals was measured from one hundred wires found in the SEM images. The crystal structure of the synthesized α-FeOOH was characterized by X-ray diffraction (XRD). The specific surface area ($m^2\ g^{-1}$) was calculated by the Brunauer–Emmett–Teller (BET) method from nitrogen adsorption–desorption isotherms, shown in Fig. S2.† The zeta potentials of aqueous suspensions of goethite (1 mg mL^{-1}) were estimated from the measured electrophoretic mobilities by the Smoluchowski model. The optical absorption spectra of α-FeOOH were recorded by using a UV-NIR spectrophotometer. A depth profile of the actual composition was studied using hard X-ray photoelectron spectroscopy (HAXPES) at two different photon energies, 2.3 keV and 6.9 keV, corresponding to mean probe depths of 30 Å and 87 Å, respectively, for the core level spectra presented.[11]

For adsorption–desorption tests, goethite powders at a concentration of 1 g mL^{-1} were dispersed in a 10 mg mL^{-1} methylene blue (MB) solution. The adsorption/desorption of the MB on the goethite was studied at different pH values. Goethite used in this study is inactive towards MB photocatalytic degradation, although part of MB is degraded through photolysis, see Fig. S3 and S4.† Powders were dispersed in the MB solution for 30 seconds with an ultrasonic device Hielscher UPS 200 (Germany) by applying the maximum power of 200 W on a 20 mL sample. After adsorption, nanowires were separated by centrifugation for 10 min at 5000 rpm. The supernatant was examined for the MB concentration by UV-Vis spectroscopy. To test for desorption, suspensions were irradiated by using a 50 mW cm^{-2} diode lamp under constant stirring (see the ESI, Fig. S5† for emission spectra). After set time intervals, MB absorption was measured in the sample aliquots. Attenuated total reflection–Fourier transform infrared (ATR-FTIR) spectra were acquired from goethite powders before MB adsorption, after MB adsorption and after visible light irradiation. For more experimental details, see the ESI.†

The precipitate consisted of nanosized goethite. Nanowires are shown in the SEM and TEM micrographs with an average length of 353 ± 49 nm, a diameter of 27 ± 5 nm and an aspect ratio up to 13, Fig. 1. XRD studies showed a single goethite phase (Fig. S6†). The specific surface area of goethite nanowires was 92.8 $m^2\ g^{-1}$.

Adsorption to nanowires is governed by goethite surface properties. Chemical uniformity or eventual radial composition gradients in the nanowires can become of significant influence with regard to the adsorption process. In order to probe the surface *versus* bulk composition, we performed HAXPES studies (Fig. 2). The O 1s HAXPES (Fig. 2 top) of the goethite sample shows peaks at binding energies typical of both hydroxyl (at 531.5 eV) and lattice oxide (at 530.2 eV) at different probe depths. A slight decrease in the ratio of the hydroxyl to the oxide peak at a larger mean probe depth (at 6.9 keV) infers that hydroxyl groups might be more abundant near the surface. The same can be observed for the magnetite reference sample, where some intensity in the energy range of the hydroxyl peak becomes weaker for a larger probe depth, and is typical of *ex situ* oxide particles, which often show some hydroxyl contents at the surface. The Fe 2p HAXPES indicates uniformly ferric (Fe^{3+}) iron in goethite, while the magnetite spectrum, given as a reference, demonstrates a typical composition gradient of multivalent oxides with a more oxidised surface layer, while the ferrous (Fe^{2+}) component being more abundant in the bulk, thus excluding the possibility for iron with different oxidation states in the synthesized goethite sample. Goethite shows no variation in the ferric signature with the probe depth. Point defects in goethite can influence adsorption properties.[12] The formation of ferrous iron in oxides and oxy-hydroxides may be triggered by the formation of oxygen vacancies because of the necessity to maintain the electrical neutrality of the crystal lattice.[13] From HAXPES, we can conclude that the goethite used in studies is more or less from point defects.

The Kubelka–Munk FTIR optical absorption spectrum showed bands centred at 650 nm and a broad absorption band in the wavelength range of 700–1000 nm, which correspond to the 6A1(6S) → 4T2(4G) and 6A1(6S) → 4T1(4G) ligand-field transitions of Fe^{3+}, see Fig. S4.† [14] The forbidden band-gap of goethite at 2.4 eV was observed from the optical absorption

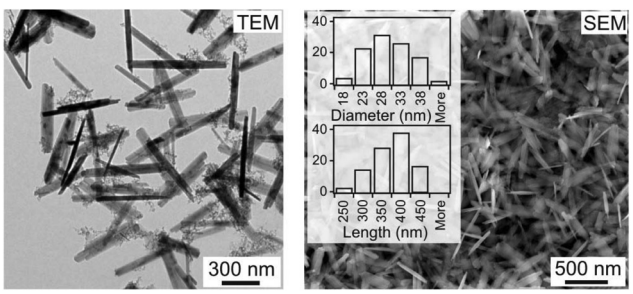

Fig. 1 Electron microscopy images and size distribution (diameter and length) of goethite nanowires.

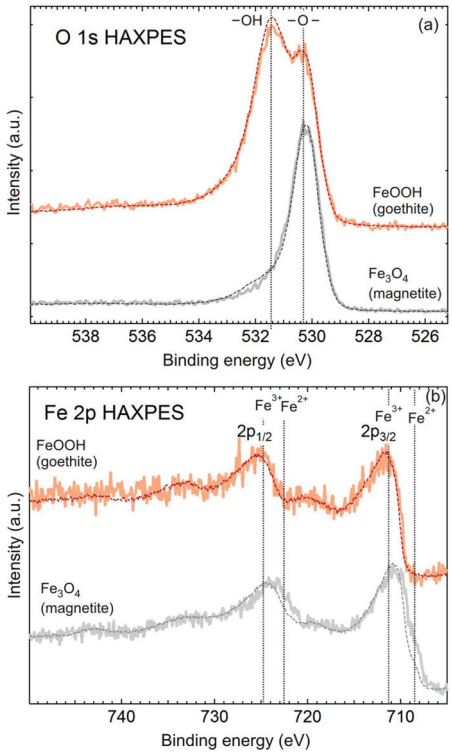

Fig. 2 HAXPES of the goethite nanowire O 1s (top) and Fe 2p (bottom) core levels, compared to a magnetite reference spectrum. Dashed and solid curves relate to different inelastic mean free paths of 30 Å and 87 Å, respectively.

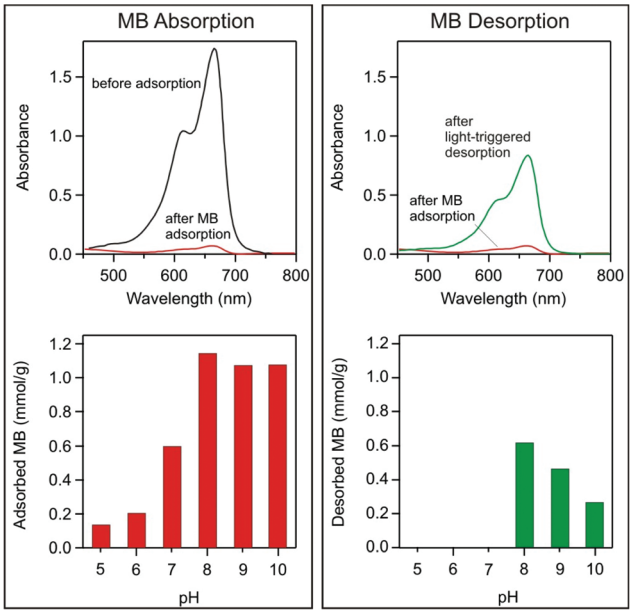

Fig. 3 Adsorption (left) and desorption (right) of MB evidenced in UV-vis spectra and quantitatively shown at different pH values. Adsorption of MB is pronounced is solutions at a pH above 7, while desorption is the most effective at pH 8. The relative error of the measured adsorbed/desorbed amount is on the order ±10%.

$(\alpha h\nu)^2$ *versus* photon energy plots (Fig. S7†), and is in good agreement with previously reported values.[8] Our synthesized goethite exhibits light absorption up to 516 nm, showing application under visible light (sunlight) conditions.

Goethite nanowires exhibit a rapid MB adsorption in the dark, which saturates within 5 minutes at pH 5–10 absorbing up to 1.14 mmol g^{-1} MB (Fig. 3 left). After subjecting the suspension to visible light irradiation, MB desorption is observed, releasing 54.1% (0.615 mmol g^{-1}) of MB in 5 hours at pH 8 (Fig. 3 right). Desorption *versus* irradiation time is plotted in Fig. S8.†

The pH of the dye solution is an important factor controlling adsorption processes, particularly the adsorption capacity. The influence of pH on MB adsorption on goethite is demonstrated in Fig. 3, where the adsorbed amount is shown at different pH values. Adsorption depends on solution pH because a higher pH increases the surface charge on goethite,[8,9] as shown from the electrokinetic measurements in Fig. S6.† In the pH range of interest, a positive charge is imparted to the MB. Considerable MB adsorption started at the isoelectric point, of pH 7, where goethite was negatively charged. An opposite charge electrostatically attracts the adsorbent to the carrier surface, thereby promoting adsorption.

Light-triggered desorption is observed in suspensions at pH values higher than the isoelectric point of pH 7 (Fig. 3). The desorption at a pH value lower than 8 may not be observed due to a low adsorbed MB concentration and possible degradation of MB *via* photolysis (see Fig. 4), and therefore, the released MB is destroyed during irradiation. However, desorption is observed in suspensions at a pH value of 8–10. Desorption is the strongest at a pH of 8 and decreases with increasing pH, Fig. 3d. The decrease in desorption could be related to a stronger attraction between the positively charged MB and the negatively charged goethite surface, as the nanowire surface becomes more negatively charged at higher pH, see Fig. S9.† During irradiation of suspension, the pH slightly decreases (Fig. S10†), which further confirms MB desorption.[15]

MB absorption–desorption on goethite nanowires was confirmed by ATR-FTIR spectroscopy measurements. Nanowires

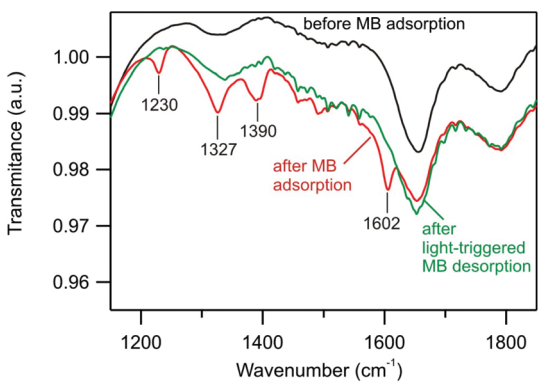

Fig. 4 ATR-FTIR spectra of goethite powder before MB adsorption, after MB adsorption, and after light-triggered MB desorption. For the full spectrum, see Fig. S11.†

were separated from suspensions by centrifugation, dried and analyzed. The goethite ATR-FTIR spectrum agrees with previous reports (ref. 15), showing intense bands at 887 cm^{-1} and 790 cm^{-1} caused by the in-plane bending of surface hydroxyl in Fe–OH–Fe and a broad band at 3133 cm^{-1} from the O–H stretching vibrations, Fig. S11.† The absorption of MB in the dark modifies the spectrum with distinguishable absorption bands at 1230 cm^{-1}, 1327 cm^{-1}, 1390 cm^{-1}, and 1602 cm^{-1} (Fig. 4).[16] These bands disappear after 5 h of light irradiation, confirming MB desorption, indicating the release of MB from goethite.

We postulate that MB desorption from light exposure is caused by local heating of individual goethite nanowires; the suspension temperature did not change from 30 °C, but is explained by the heat capacity of the large volume of water. During visible light absorption, photo-generated electrons and holes are known to recombine and release light energy as heat.[17] To confirm this release mechanism, we heated goethite suspensions with the adsorbed MB in the dark and observed desorption of MB. Almost no desorption was detected at a temperature of 30 °C, while at 70 °C considerable desorption in the dark was observed, see Fig. S8.† Therefore, we conclude that the light energy on goethite locally heated heats the nanowires and triggers the desorption of MB.

Other effects like goethite surface dissolution can be ruled out also because no dissolution was observed under 2.4-fold higher UV-vis light intensity in the same irradiation duration.[9] The surface changes of the goethite in the presence of H_2O_2 or polycarboxylic acids as a rule are going alongside with the generation of reactive oxygen species which attack the organic molecules. In the present work, methylene blue release has been observed without adding any promoters for the goethite surface change in light.

In order to test the recycling potential for the adsorption/desorption process, we collected, washed, and dried the goethite powder and repeated the adsorption–desorption process. Goethite adsorption and desorption over regenerated α-FeOOH nanowires is demonstrated in Fig. S13.† In the 2nd cycle, the adsorbed MB amount at pH = 8 reached 0.92 mmol g^{-1} and after 5 hours of visible light irradiation, 0.24 mmol g^{-1} (27%) was desorbed. Although a drop in the adsorbed and desorbed amount after recycling was observed, these experiments confirm the possibility of the regeneration of the material.

In conclusion, we have shown visible light-triggered MB desorption from goethite nanowires. The desorption of MB in visible light is most pronounced at a pH just above the isoelectric point where MB absorption is weaker, allowing easier separation. The light-triggered desorption of MB is caused by nanowire local heating, shifting the adsorption–desorption equilibrium towards desorption. The reported phenomenon provides new possibilities for preparing light responsive materials, and enables new applications that benefit from a simple light trigger. Furthermore, due to the non-destructive nature of the process, recycling and regeneration can be performed.

Conflicts of interest

There are no conflicts of interest to declare.

Acknowledgements

This work has been supported by the European Regional Development Fund within the Activity 1.1.1.2 “Post-doctoral Research Aid” of the Specific Aid Objective 1.1.1 “To increase the research and innovative capacity of scientific institutions of Latvia and the ability to attract external financing, investing in human resources and infrastructure” of the Operational Programme “Growth and Employment” (No. 1.1.1.2/VIAA/1/16/157) and by the Estonian Research Council fund projects PUT1096, IUT2-25. G. T. acknowledges the support from University of Geneva and Swiss National Science Foundation. We are grateful to the staff of BESSY II for the assistance and co-operation during the synchrotron-based measurements and the financial support of HZB.

References

1 H. Kim, H. Lee, K.-Y. Seong, E. Lee, S. Y. Yang and J. Yoon, Visible Light-Triggered On-Demand Drug Release from Hybrid Hydrogels and Its Application in Transdermal Patches, *Adv. Healthcare Mater.*, 2015, **4**(14), 2071–2077, DOI: 10.1002/adhm.201500323.

2 J. Xu, X. Zhou, Z. Gao, Y.-Y. Song and P. Schmuki, Visible-Light-Triggered Drug Release from TiO2 Nanotube Arrays: A Controllable Antibacterial Platform, *Angew. Chem., Int. Ed.*, 2016, **55**(2), 593–597, DOI: 10.1002/anie.201508710.

3 R. Gao, D. Cao, Y. Guan and D. Yan, Flexible Self-Supporting Nanofibers Thin Films Showing Reversible Photochromic Fluorescence, *ACS Appl. Mater. Interfaces*, 2015, **7**(18), 9904–9910, DOI: 10.1021/acsami.5b01996.

4 S. Li and D. Yan, Tuning Light-Driven Motion and Bending in Macroscale-Flexible Molecular Crystals Based on a Cocrystal Approach, *ACS Appl. Mater. Interfaces*, 2018, **10**(26), 22703–22710, DOI: 10.1021/acsami.8b05804.

5 Z. Li, R. Liang, S. Xu, W. Liu, D. Yan, M. Wei, D. G. Evans and X. Duan, Multi-Dimensional, Light-Controlled Switch of Fluorescence Resonance Energy Transfer Based on Orderly Assembly of 0D Dye@micro-Micelles and 2D Ultrathin-Layered Nanosheets, *Nano Res.*, 2016, **9**(12), 3828–3838, DOI: 10.1007/s12274-016-1252-1.

6 Z. Li, R. Liang, W. Liu, D. Yan and M. Wei, A Dual-Stimuli-Responsive Fluorescent Switch Ultrathin Film, *Nanoscale*, 2015, **7**(40), 16737–16743, DOI: 10.1039/C5NR05376E.

7 B. Lv, Z. Wu, C. Ji, W. Yang, D. Yan and M. Yin, Spiropyran-Induced One-Dimensional Cyclodextrin Microcrystals with Light-Driven Fluorescence Change, *J. Mater. Chem. C*, 2015, **3**(33), 8519–8525, DOI: 10.1039/C5TC01817J.

8 C. Ruales-Lonfat, J. F. Barona, A. Sienkiewicz, M. Bensimon, J. Vélez-Colmenares, N. Benítez and

C. Pulgarín, Iron Oxides Semiconductors Are Efficients for Solar Water Disinfection: A Comparison with Photo-Fenton Processes at Neutral PH, *Appl. Catal., B*, 2015, **166–167**, 497–508, DOI: 10.1016/j.apcatb.2014.12.007.

9 P. M. Borer, B. Sulzberger, P. Reichard and S. M. Kraemer, Effect of Siderophores on the Light-Induced Dissolution of Colloidal Iron(III) (Hydr)Oxides, *Mar. Chem.*, 2005, **93**(2), 179–193, DOI: 10.1016/j.marchem.2004.08.006.

10 P. Borer and S. J. Hug, Photo-Redox Reactions of Dicarboxylates and α-Hydroxydicarboxylates at the Surface of Fe(III)(Hydr)Oxides Followed with in Situ ATR-FTIR Spectroscopy, *J. Colloid Interface Sci.*, 2014, **416**, 44–53, DOI: 10.1016/j.jcis.2013.10.030.

11 F. Schäfers, The Crystal Monochromator Beamline KMC-1 at BESSY II, *J. Large-Scale Res. Facil.*, 2016, **2**, 96, DOI: 10.17815/jlsrf-2-92.

12 Y. Cao, L. Shen, X. Hu, Z. Du and L. Jiang, Low Temperature Desulfurization on Co-Doped α-FeOOH: Tailoring the Phase Composition and Creating the Defects, *Chem. Eng. J.*, 2016, **306**, 124–130, DOI: 10.1016/j.cej.2016.07.047.

13 A. Šutka and K. A. Gross, Spinel Ferrite Oxide Semiconductor Gas Sensors, *Sens. Actuators, B*, 2016, **222**, 95–105, DOI: 10.1016/j.snb.2015.08.027.

14 D. M. Sherman and T. D. Waite, Electronic Spectra of Fe3 + Oxides and Oxide Hydroxides in the near IR to near UV, *Am. Mineral.*, 1985, **70**(11–12), 8.

15 E. Gurr, PH of Ionic Dye Solutions, *Nature*, 1964, **202**(4935), 920, DOI: 10.1038/202920a0.

16 O. V. Ovchinnikov, A. V. Evtukhova, T. S. Kondratenko, M. S. Smirnov, V. Y. Khokhlov and O. V. Erina, Manifestation of Intermolecular Interactions in FTIR Spectra of Methylene Blue Molecules, *Vib. Spectrosc.*, 2016, **86**, 181–189, DOI: 10.1016/j.vibspec.2016.06.016.

17 T. Berger, O. Diwald, E. Knözinger, M. Sterrer and Y. T. Yates Jr., UV Induced Local Heating Effects in TiO_2 Nanocrystals, *Phys. Chem. Chem. Phys.*, 2006, **8**(15), 1822–1826, DOI: 10.1039/B517107E.

